

Nematic Phase of the n -Component Cubic-Spin Spin Glass in $d=3$: Liquid-Crystal Phase in a Dirty Magnet

E. Can Artun,^{1,2} Deniz Sarman,³ and A. Nihat Berker^{2,1,4}

¹*TÜBİTAK Research Institute for Fundamental Sciences, Gebze, Kocaeli 41470, Turkey*

²*Faculty of Engineering and Natural Sciences, Kadir Has University, Cibali, Istanbul 34083, Turkey*

³*Department of Physics, Boğaziçi University, Bebek, Istanbul 34342, Turkey*

⁴*Department of Physics, Massachusetts Institute of Technology, Cambridge, Massachusetts 02139, USA*

A nematic phase, previously seen in the $d = 3$ classical Heisenberg spin-glass system, occurs in the n -component cubic-spin spin-glass system, between the low-temperature spin-glass phase and the high temperature disordered phase, for number of components $n \geq 3$, in spatial dimension $d = 3$, thus constituting a liquid-crystal phase in a dirty (quenched-disordered) magnet. This result is obtained from renormalization-group calculations that are exact on the hierarchical lattice and, equivalently, approximate on the cubic spatial lattice. The nematic phase completely intervenes between the spin-glass phase and the disordered phase. The Lyapunov exponents of the spin-glass chaos are calculated from $n = 1$ up to $n = 12$ and show odd-even oscillations with respect to n .

I. CUBIC-SPIN SPIN-GLASS SYSTEM AND NEMATIC PHASE IN A DIRTY MAGNET

Spin-glass systems have an inherent quantifiable chaos under scale change [1–4] and thus provide a universal classification and clustering scheme for complex phenomena [5], as well as rich ordering phenomena such as spin-glass sponge ordering [6]. Spin-glass studies have been done overwhelmingly with Ising $s_i = \pm 1$ spins. However, a recent study [7] with classical Heisenberg spins \vec{s}_i that can continuously point in 4π steradians found, instead of spin-glass order, nematic order, meaning a liquid-crystal phase in a dirty magnet. In the current study, we continue in this direction, studying n -component cubic-spin spin-glasses. Cubic spins can be considered as discretized and systematically extended versions of Heisenberg spins.

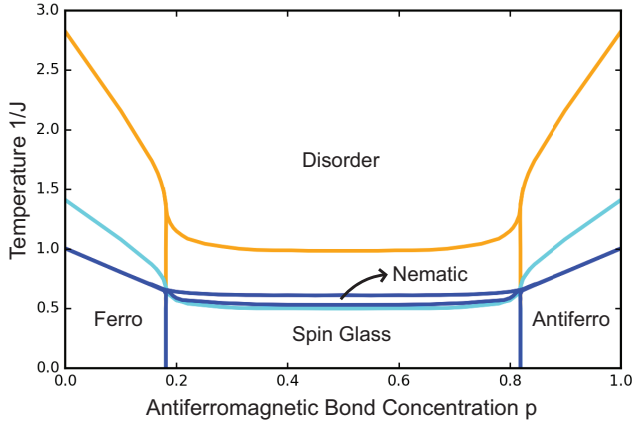


FIG. 1. Calculated phase diagrams for the cubic-spin spin-glass systems in spatial dimension $d = 3$. The phase diagrams are, from top to bottom, for number of components $n = 1, 2, 3$ components, meaning $2n$ states. A nematic phase appears for $n = 3$, persisting for $n \geq 3$, as seen in Fig.2.

The n -component cubic-spin spin-glass system is de-

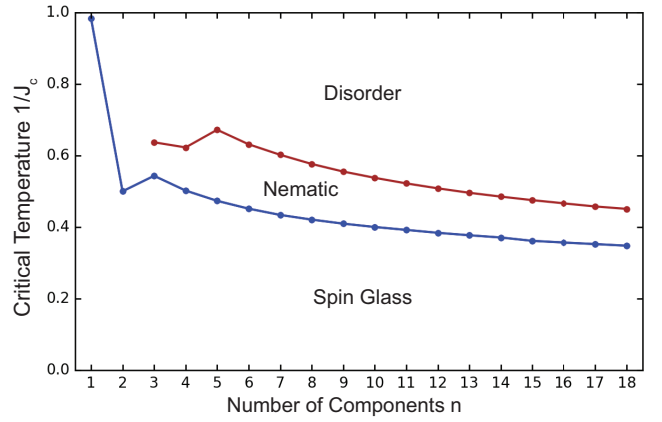


FIG. 2. Nematic and spin-glass transition temperatures at the ferro-antiferro symmetric value of $p = 0.5$, as a function of the number n of spin components. It is seen that the nematic phase persists in $n \geq 3$.

finied by the usual Hamiltonian, where $\beta = 1/kT$,

$$-\beta\mathcal{H} = \sum_{\langle ij \rangle} J_{ij} \vec{s}_i \cdot \vec{s}_j \equiv \sum_{\langle ij \rangle} -\beta\mathcal{H}_{ij}, \quad (1)$$

but where \vec{s}_i can be in $2n$ different states $\pm\hat{u}$ at each site i , \hat{u} being a unit Cartesian vector. The sum is over nearest-neighbor pairs of site $\langle ij \rangle$. The interaction J_{ij} is ferromagnetic $+J > 0$ or antiferromagnetic $-J$ with probabilities $1 - p$ and p , respectively.

The cubic-spin spin-glass system studied in this work is of particular interest, because it generalizes the much studied single-component simple spin Ising model to a realistic vector-spin system with n vector components. It is a rich system, since each of the n -component systems has phase transition behavior in a different universality class. As seen below, it is readily treatable by renormalization-group theory, yielding the complex novel result of a band of liquid-crystal phase above the spin-glass phase. This means a liquid-crystal phase occurring in a dirty magnet.

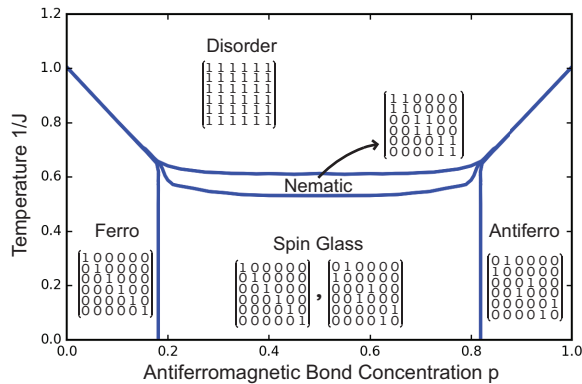


FIG. 3. Renormalization-group sinks of the phases for $n = 3$. The sink fixed-point values of the nearest-neighbor Hamiltonian exponentiated, namely the transfer matrix, are shown. All points in a given phase flow, under renormalization-group, to its corresponding sink, which epitomizes the ordering of the phase. Except for the spin-glass phase, all phases flow to their respective single transfer matrix, shown in this figure. The spin-glass phase flows to a fixed distribution of diverging ferromagnetic and antiferromagnetic interactions, shown in Fig. 4. This fixed-point structure in this Fig. 3, underpinning the phase diagrams, occurs for all $n \geq 3$.

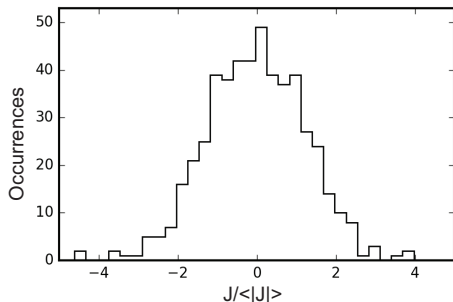


FIG. 4. The fixed distribution of the sink of the spin-glass phase. The interaction J is extracted from the 2×2 transfer matrix of the spin component \hat{u} that shows spin-glass order.

II. EXACTLY SOLVED HIERARCHICAL MODEL AND EQUIVALENT MIGDAL-KADANOFF PROCEDURE

The Migdal-Kadanoff approximation [8, 9] and its algebraically equivalent, exactly solved hierarchical model [3, 10–12] has been extensively described elsewhere. Operationally, this renormalization-group transformation consists in decimating inside b bonds in series and then adding b^{d-1} decimated bonds in parallel, where b is the length-rescaling factor ($b = 3$ in this work). It is a very simply done, very effective, and most extensively used [5, 13–22] renormalization-group transformation. For quenched-random systems, as in the present work, starting with a large distribution (of 10,000 realizations in this work), a renormalized distribution is generated by randomly associating b^d nearest-neighbor terms,

10,000 times. This is the solution of an actual physical realization.[23–26] Following the renormalization-group trajectories of the distributions, the phases and phase boundaries are obtained, as shown below. Thus, our analysis is done by analyzing the renormalization-group trajectories of 20,000 interactions, which is a gigantic calculation.

The transformation is best implemented algebraically by writing the exponentiated nearest-neighbor Hamiltonian, namely the transfer matrix between two neighboring sites, namely

$$\mathbf{T}_{ij} \equiv e^{-\beta \mathcal{H}_{ij}} = e^{J \vec{s}_i \cdot \vec{s}_j} = \begin{pmatrix} e^J & e^{-J} & 1 & 1 & 1 & 1 \\ e^{-J} & e^J & 1 & 1 & 1 & 1 \\ 1 & 1 & e^J & e^{-J} & 1 & 1 \\ 1 & 1 & e^{-J} & e^J & 1 & 1 \\ 1 & 1 & 1 & 1 & e^J & e^{-J} \\ 1 & 1 & 1 & 1 & e^{-J} & e^J \end{pmatrix}, \quad (2)$$

where the consecutive states are plus and minus directions of the sequence of cartesian unit vectors \hat{u} . The transfer matrix is given here for $n = 3$ components. The generalization to arbitrary n is obvious, and used in this work. The decimation step consists in matrix-multiplying b transfer matrices. The bond-moving step consists in taking, after decimation, the power of b^{d-1} of each element in the transfer matrix. Here b is the length-rescaling factor of the renormalization-group transformation.

III. EMERGENT NEMATIC PHASE IN CALCULATED PHASE DIAGRAMS

Calculated phase diagrams are shown in Fig. 1, for the cubic-spin spin-glass systems in spatial dimension $d = 3$. The phase diagrams are for number of components $n = 1, 2, 3$, meaning $2n$ states. A nematic phase appears for $n = 3$, persisting for $n \geq 3$, as seen in Fig.2. The renormalization-group sinks of the phases are shown in Fig. 3 for $n = 3$. The sink fixed-point values of the nearest-neighbor Hamiltonian exponentiated, namely the transfer matrix, Eq. (2), are shown. All points in a given phase flow, under renormalization-group, to its corresponding sink, which epitomizes the ordering of the phase. Except for the spin-glass phase, all phases flow to their respective single transfer matrix, shown in this figure. The spin-glass phase flows to a fixed distribution of diverging ferromagnetic and antiferromagnetic interactions, shown in Fig. 4.

The renormalization-group trajectories starting in a given phase unmistakably reach their respective sinks within 8 renormalization-group iterations, including the case of the nematic phase. Renormalization-group trajectories starting close to a phase boundary spend iterations close to the unstable fixed point controlling the phase boundary, but reach the sink within 15 iterations

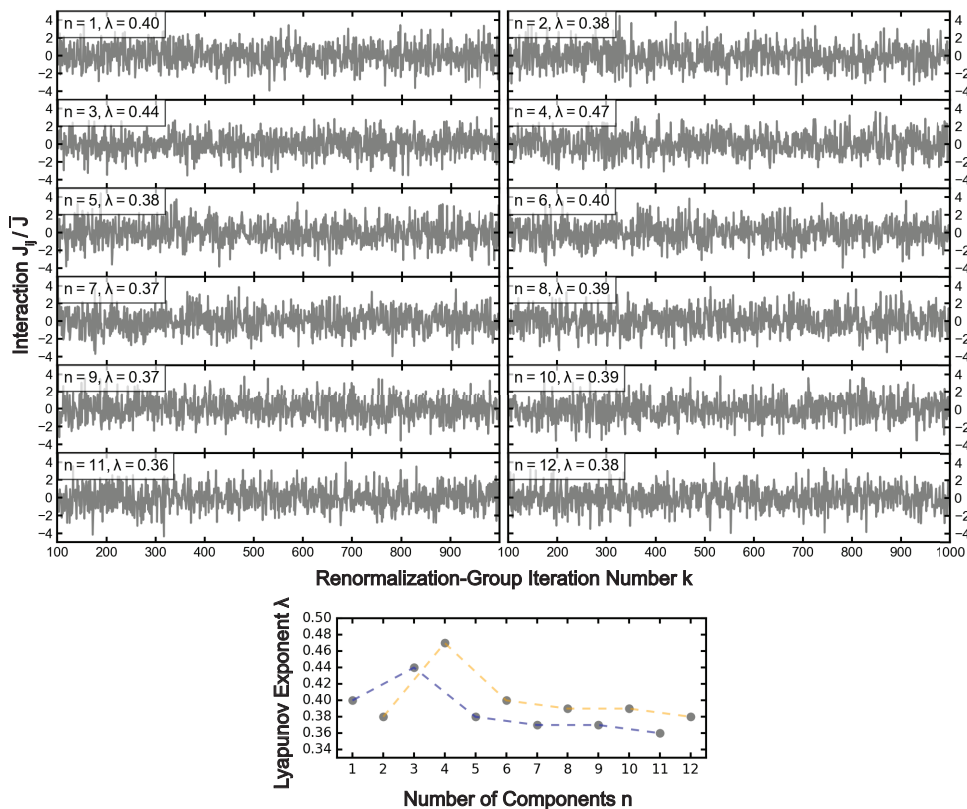


FIG. 5. Chaotic renormalization-group trajectories of the spin-glass phases and their Lyapunov exponents. The Lyapunov exponents show odd-even oscillations with respect to the number of cubic components n .

for the accuracy of our calculation. The calculational uncertainty in our work is smaller than the thickness of all of the phase boundary lines in our figures.

The renormalization-group trajectories in the spin-glass phase are chaotic, as shown in Fig. 5. The strength of chaos under scale change [1–4] is measured by the Lyapunov exponent [27, 28],

$$\lambda = \lim_{n \rightarrow \infty} \frac{1}{n} \sum_{k=0}^{n-1} \ln \left| \frac{dx_{k+1}}{dx_k} \right|, \quad (3)$$

where $x_k = J_{ij}/\bar{J}$ at step k of the renormalization-group trajectory and \bar{J} is the average of the absolute value of the interactions in the quenched random distribution. We calculate the Lyapunov exponents by discarding the first 100 renormalization-group steps (to eliminate crossover from initial conditions to asymptotic behavior) and then using the next 900 steps, shown in Fig. 5. The initial (J) values do not matter, as long as they are within the specified spin-glass phase. As seen in Fig. 5, the calculated Lyapunov exponents show odd-even oscillations with respect to the number of cubic components n . Such oscillations have been seen previously, for example, as a function of spin s value, in critical temperatures of the Ising magnet.[29]

In addition to chaos, the renormalization-group trajec-

tories show asymptotic strong-coupling behavior [30],

$$\bar{J} = b^{y_R} \bar{J}, \quad (4)$$

where $y_R > 0$ is the strong-coupling runaway exponent [30]. Again using 900 renormalization-group steps after discarding 100 steps, we calculated the runaway exponent and find the same value of $y_R = 0.24$ for all n . The fact that y_R is much less than $d - 1 = 2$ shows that this spin-glass order in very unsaturated order. In the compact (saturating) ordering of systems without quenched randomness, $y_R = d - 1$ reflects the energy of the smooth interface between oppositely aligned renormalization-group cells.[31]

The sink values of the nematic phase shows that the system aligns along one of the $\pm \hat{u}$, irrespective of the plus or minus direction, which is a nematic phase. This is a spin-space discretized version of the nematic phase in the classical Heisenberg spin-glass system, where the nematic alignment is along one of the continuum of 4π steradians, again irrespective of \pm direction. The nematic phase intercedes, along the entire length, between the low-temperature spin-glass phase and the high-temperature disordered phase. This renormalization-group and phase diagram picture, detailed here for $n = 3$, occurs for all $n \geq 3$.

IV. CONCLUSION

We have calculated the phase diagram of the cubic-spin spin-glass system in $d = 3$. We find that a nematic phase, such as seen in the classical Heisenberg model with continuously orientable spins, emerges from the chaotic spin-glass phase, for number of component $n \geq 3$. The calculated Lyapunov exponents λ , measuring the strength of the spin-glass chaos, show odd-even oscillations with re-

spect to the number of cubic spin components n , whereas the strong-coupling runaway exponent y_R has the same low value of $0.24 \ll d - 1 = 2$ for all n , showing the much unsaturated order of the spin-glass phase.

ACKNOWLEDGMENTS

Support by the Kadir Has University Doctoral Studies Scholarship Fund and by the Academy of Sciences of Turkey (TÜBA) is gratefully acknowledged.

-
- [1] S. R. McKay, A. N. Berker, and S. Kirkpatrick, Spin-Glass Behavior in Frustrated Ising Models with Chaotic Renormalization-Group Trajectories, *Phys. Rev. Lett.* **48**, 767 (1982).
- [2] S. R. McKay, A. N. Berker, and S. Kirkpatrick, Amorphously Packed, Frustrated Hierarchical Models: Chaotic Rescaling and Spin-Glass Behavior, *J. Appl. Phys.* **53**, 7974 (1982).
- [3] A. N. Berker and S. R. McKay, Hierarchical Models and Chaotic Spin Glasses, *J. Stat. Phys.* **36**, 787 (1984).
- [4] S. R. McKay and A. N. Berker, *J. Appl. Phys.*, Chaotic Spin Glasses: An Upper Critical Dimension, *J. Appl. Phys.* **55**, 1646 (1984).
- [5] E. C. Artun, I. Keçoğlu, A. Türkoğlu, and A. N. Berker, Multifractal Spin-Glass Chaos Projection and Interrelation of Multicultural Music and Brain Signals, *Chaos, Solitons, Fractals* **167**, 113005 (2023).
- [6] Y. E. Pektaş, E. C. Artun, and A. N. Berker, Driven and Non-Driven Surface Chaos in Spin-Glass Sponges, *Chaos, Solitons, Fractals* **176**, 114159 (2023).
- [7] E. Tunca and A. N. Berker, Nematic Ordering in the Heisenberg Spin-Glass System in $d = 3$ Dimensions, *Phys. Rev. E* **107**, 014116 (2023).
- [8] A. A. Migdal, Phase transitions in gauge and spin lattice systems, *Zh. Eksp. Teor. Fiz.* **69**, 1457 (1975) [*Sov. Phys. JETP* **42**, 743 (1976)].
- [9] L. P. Kadanoff, Notes on Migdal's recursion formulas, *Ann. Phys. (N.Y.)* **100**, 359 (1976).
- [10] A. N. Berker and S. Ostlund, Renormalisation-Group Calculations of Finite Systems: Order Parameter and Specific Heat for Epitaxial Ordering, *J. Phys. C* **12**, 4961 (1979).
- [11] R. B. Griffiths and M. Kaufman, Spin Systems on Hierarchical Lattices: Introduction and Thermodynamic Limit, *Phys. Rev. B* **26**, 5022R (1982).
- [12] M. Kaufman and R. B. Griffiths, Spin Systems on Hierarchical Lattices: 2. Some Examples of Soluble Models, *Phys. Rev. B* **30**, 244 (1984).
- [13] J. Clark and C. Lochridge, Weak-Disorder Limit for Directed Polymers on Critical Hierarchical Graphs with Vertex Disorder, Stochastic Processes and Their Applications **158**, 75 (2023).
- [14] M. Kotorowicz and Y. Kozitsky, Phase Transitions in the Ising Model on a Hierarchical Random Graph Based on the Triangle, *J. Phys. A*, **55**, 405002 (2022).
- [15] P.-P. Zhang, Z.-Y. Gao, Y.-L. Xu, C.-Y. Wangmand X.-M. Kong, Phase Diagrams, Quantum Correlations and Critical Phenomena of Antiferromagnetic Heisenberg Model on Diamond-Type Hierarchical Lattices, *Quantum Science and Technology* **7**, 025024 (2022).
- [16] K. Jiang, J. Qiao, and Y. Lan, Chaotic Renormalization Flow in the Potts model induced by long-range competition, *Phys. Rev. E* **103**, 062117 (2021).
- [17] I. Chio and R. K. W. Roeder, Chromatic Zeros on Hierarchical Lattices and Equidistribution on Parameter Space, *Annales Inst. Henri Poincaré D* **8**, 491 (2021).
- [18] A. V. Myshlyavtsev, M. D. Myshlyavtseva, and S. S. Akimenko, Classical Lattice Models with Single-Node Interactions on Hierarchical Lattices: The Two-Layer Ising Model, *Physica A* **558**, 124919 (2020).
- [19] M. Derevyagin, G. V. Dunne, G. Mograby, and A. Teplyaev, Perfect Quantum State Transfer on Diamond Fractal Graphs, *Quantum Information Processing*, **19**, 328 (2020).
- [20] S.-C. Chang, R. K. W. Roeder, and R. Shrock, q-Plane Zeros of the Potts Partition Function on Diamond Hierarchical Graphs, *J. Math. Phys.* **61**, 073301 (2020).
- [21] C. Monthus, Real-Space Renormalization for Disordered Systems at the Level of Large Deviations, *J. Stat. Mech. - Theory and Experiment*, 013301 (2020).
- [22] O. S. Sariyer, Two-Dimensional Quantum-Spin-1/2 XXZ Magnet in Zero Magnetic Field: Global Thermodynamics from Renormalisation Group Theory, *Philos. Mag.* **99**, 1787 (2019).
- [23] R. H. Kraichnan, Dynamics of Nonlinear Stochastic Systems, *J. Math. Phys.* **2**, 124 (1961).
- [24] P. J. Flory, *Principles of Polymer Chemistry* (Cornell University Press: Ithaca, NY, USA, 1986).
- [25] M. Kaufman, Entropy Driven Phase Transition in Polymer Gels: Mean Field Theory, *Entropy* **20**, 501 (2018).
- [26] P. Lloyd and J. Oglesby, Analytic Approximations for Disordered Systems, *J. Phys. C: Solid St. Phys.* **9**, 4383 (1976).
- [27] P. Collet and J.-P. Eckmann, *Iterated Maps on the Interval as Dynamical Systems* (Birkhäuser, Boston, 1980).
- [28] R. C. Hilborn, *Chaos and Nonlinear Dynamics*, 2nd ed. (Oxford University Press, New York, 2003).
- [29] A. N. Berker, Critical Interactions for the Triangular Spin-s Ising Model by a Spin-Restructuring Transformation, *Phys. Rev. B* **12**, (1975).
- [30] M. Demirtaş, A. Tuncer, and A. N. Berker, Lower-Critical Spin-Glass Dimension from 23 Sequenced Hierarchical Models, *Phys. Rev. E* **92**, 022136 (2015).

- [31] A. N. Berker and M. Wortis, Blume-Emery-Griffiths-Potts Model in Two Dimensions: Phase Diagram and Critical Properties from a Position-Space Renormalization Group, *Phys. Rev. B* **14**, 4946 (1976).